A Dynamic Model and Turning Strategy of a Laterally-Tiltable and Self-Balancing Two-Wheeled Robot

Wei-Shun Yu and Pei-Chun Lin

***Abstract*—This paper describes the development of a two-wheel balancing robot capable of actively changing its posture in the lateral direction to facilitate the turning motion. The work includes the development of a mechanism and the control strategy for both self-balancing and lateral motion control. The dynamic model of the robot was developed using the Lagrangian approach, and it was utilized as the plant of the motion controller. To validate the performance of the tiltable design and controller of the robot, the robot was experimentally evaluated, and its performance was compared to that of the robot without using the tiltable mechanism.**

keywords: Two-wheeled robot, Self-balancing, dynamic, tiltable, mechanism

I. INTRODUCTION

IN the past few years, many teams studied the dynamic model and controller design of self-balancing two-wheeled robots. The model of a self-balancing two-wheeled robot could be simplified to an inverted pendulum system, a classic control topic. It has been discussed in the academic field and specialized in its model or control theory improvement for different functions. The theory of dynamic balance was first proposed by Japanese scholars in 1994 [1, 2]. The platform achieved self-balancing and movement on a 2-D plane using the Lagrange equation to derive a model and pole placement controller.

The most famous work of self-balancing two-wheeled robots in the academic field is JOE [3], published by German scholars in 2002. It analyzed the dynamic model using Newtonian mechanics and linearized the non-linear at the lateral axis of the two-wheel. They also design a control system consisting of two decoupled state-space controllers for balancing the robot and turning. JOE could move stable at 1.5m/s and travel on a 30-degree inclined plane. We find that most self-balancing two-wheeled robot linearize their model at a pitch angle of around 0 and design their controller [4-6]. Different controllers adapt to the external environment and adjust their control parameters to achieve more stable control. For example, an adaptive neural network controller could adjust balancing control parameters to achieve more stable movement [7]. Some controllers are used to achieve different controller targets for the non-linear part of the dynamic model. Using sliding mode control (SMC) handles disturbances [8] or improves pose change performance [9]. On-line adaptive PID controllers overcome parameter variations [10]. A fuzzy controller achieves travel and position control [11] or finds better control gain [12]. In the commercial market, some vehicles utilize two-wheel inverted pendulums as a mode of mobility. A well-known example is the Segway [13], a personal transporter designed by DEKA company in 2001. Segway could achieve stable forward movement by balancing through multiple gyroscopes. Users could control the forward speed of the vehicles through their pitch angle without keeping the vehicle balanced. However, due to vehicle regulations in various countries and high unit prices, Segway has not received a positive response as a product. However, it still inspired the development of personal vehicles.

In recent years, personal vehicles have been considered a solution to individual transportation systems in the 21st century [14]. These vehicles typically feature narrow and tall to apply in original human space. However, a relatively high center of mass means it is easy to overturn when receiving lateral force when turning. So, an active tilt degree of freedom has been considered a possible solution in the academic field. Commonly, these narrow and tall vehicles with active tilt degrees of freedom are referred to as narrow-tilting vehicles (NTV) in the academic field. Johl et al. designed a three-wheeled tilt mobile and developed a controller by linearizing its dynamic model [15]. Chiou and Chen designed a four-wheeled NTV with wheels arranged in a diamond configuration and developed its mode as a planar multibody system [16]. Kwon et al. also designed a tiltable robot [17]. Pham et al. developed a balancing ballbot [18].

The main target of NTV tilting control is to stabilize the tilting mode so that users can proceed along a predefined trajectory and minimize the torque required to drive the tilting degree of freedom. The control methods can be divided into direct tilt control (DTC) and steering tilt control (STC). DTC adjusts the tilt angle according to the external state, affecting turning characteristics such as rotational radius, lateral acceleration, tangential speed, etc. DTC simplifies the design of the control system but requires more torque when speed changes. STC controls the whole system by steer-by-wire, so the steering angle from users is the primary input and is used to decide the tilting angle. STC makes it easier for users to track their desired movement trajectory [15, 19, 20] but needs more torque at low speeds. Due to the different application characteristics of DTC and STC, some methods that combine STC and DTC have also been studied in the academic field. Rajamani et al. designed a tilt brake system that could combine the advantages of DTC and STC [21]. Optimizing the tilt controller in the frequency domain to reduce the transient performance and improve the STC was also presented [22]. However, relatively few teams studied the combination of self-balancing and tilt angle control. Most of the focus is on mechanism design and dynamics behavior. Korea Aerospace University developed a two-wheeled robot with two symmetrical mechanism modules [23]. A rack-pinion mechanism mounted between two modules could achieve active

Manuscript received 15 April 2024; revised 5 June 2024; accepted 6 June; Date of publication 17 June 2024. This work is supported by the National Science and Technology Council (NSTC), Taiwan, under contract NSC 99-2218-E-002-012- and MOST 110-2221-E-002 -111 -MY3. (*Corresponding author: Pei-Chun Lin*)

The authors are with the Department of Mechanical Engineering, National Taiwan University, Taipei 10617, Taiwan (e-mail: r99522806@ntu.edu.tw; peichunlin@ntu.edu.tw).

tilting motion. Muñoz-Hernandez et al. developed an attitude control of a two-wheel self-balancing robot [24].

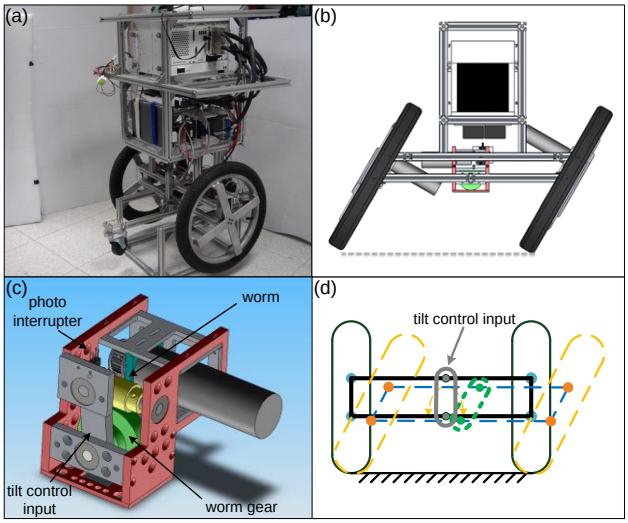

Fig. 1. The laterally-tiltable and self-balancing two-wheeled robot: (a) Photo of the robot, (b) the configuration of the robot in tilt, (c) the actively controllable tilt mechanism, (d) the illustrative drawing of the robot in normal and tilted postures.

This paper provides a mechanism design of a tilt platform that could lower tilt control power. According to the tilt mechanism design, a dynamic model of a two-wheeled robot with an additional tilt degree of freedom is proposed to analyze the influence of tilt degree on self-balancing behavior by both simulation and experiment. Meanwhile, the tilt mechanism is used to design a turning strategy with different tilt angles.

The rest of the article is organized as follows. Section II describes the tilt mechanism design. Section III reports the dynamic model of a two-wheeled self-balancing robot model. Section IV shows experiment validation of self-balancing and tilt angle control and develops a tilt-turning strategy. Section V shows turning results between traditional voltage control and tilt turning strategy. Section VI concludes this article.

II. Mechanism Design of the Laterally Tiltable Robot

Mobility and agility are the main advantages of a two-wheeled mobile robot. However, lateral overturning would be relatively easy when the platform turns while traveling at a high speed because of a high center of mass. Lowering the center of mass could improve this issue.

We develop a mechanism to reduce the center of mass by tilting the robot body. Wheel actuator modules and tilting mechanism are connected by parallel four-bar linkage, as shown in Fig. 1(a). The tilting mechanism could control the four-bar linkage and the whole body of the mobile robot, as shown in Fig. 1(b). A worm drive system was utilized as the tilting control mechanism, as shown in Fig. 1(c). The motor's power is transmitted from a set of pulleys to a shaft coaxial with a worm. Then, the worm drive system would transmit power to tilt the control input linkage to tilt the four-bar linkage to accomplish lateral movement of the mobile robot body. Meanwhile, this design could maintain a stable tilting angle without extra power or control of the non-back drivable feature of the worm drive system. To ensure that the mobile platform remains level with the ground throughout the tilting process, the angle between the wheel and the ground should follow the angle input of the tilt input bar. We make wheel actuator modules located in the middle of the wheels, as shown in Fig. 1(d). The final design could achieve a control tiling angle range of ±20 degree. And the actual mechanism design values are shown in TABLE I

TABLE I
THE MECHANISM DESIGN VALUES OF THE ROBOT

Symbol	Definition	Value
M	Mass of robot body (Kg)	27.05
J_p	Pitch momentum of inertia of robot body (kgm^2)	0.54
l	Distance between wheel axis and CoM(m)	0.25
J_ϕ	Yaw momentum of inertia of robot body (kgm^2)	1.10
m	Mass of wheel(Kg)	1.06
r	Radius of wheel(m)	0.2
J_w	Pitch momentum of inertia of wheel(kgm^2)	0.04
n	Gear ratio of motor	36
J_m	Pitch momentum of inertia of motor(kgm^2)	1.38*10^{-5}
K_b	Back EMF constant of motor (Volt*sec/rad)	0.03
R_m	Motor inner resistor(ohm)	0.32

III. Dynamics Model of the Robot

A self-balancing two-wheeled mobile robot could be generally simplified into an inverted pendulum model. However, it would cause the effect of centripetal acceleration by increasing the distance between the center of mass and the wheel axis. Besides, the motors of two-wheeled mobile robots must balance the body posture and achieve forward movement simultaneously, increasing the difficulty of turning control. Thus, we add a tilting degree of freedom into a two-wheeled balancing dynamic model.

First, we add a tilt degree of freedom to a general self-balancing two-wheeled 3D model based on the formulation reported in [25]. The simplified system is shown in Fig. 2. The tilt system utilizes a 4-bar linkage, and the tilt angle is a control input of the system. Dynamic modeling would follow two assumptions: First, we assume that there would not be any slip of wheels when the body tilts, which means the wheel would rotate around the contact point as the axis. Second, the body's center of mass and moment of inertia would not change when tilting happens.

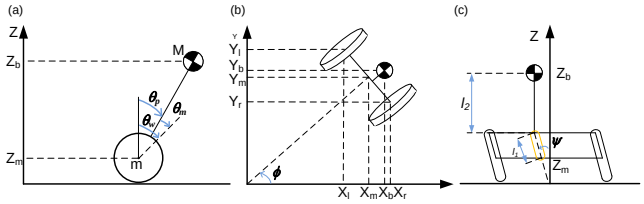

Fig. 2. The simplified inverted pendulum model of the robot: (a) side view, (b) top view, and (c) front view.

The dynamics modeling symbols are shown in TABLE I and TABLE II.

The wheel states in the world frame could be presented as

$$(\theta_w, \phi) = (\tfrac{1}{2}(\theta_{w,r} + \theta_{w,l}), \tfrac{r}{w}(\theta_{w,r} - \theta_{w,l})) \tag{1}$$

TABLE II
THE SYMBOLS OF THE DYNAMIC MODEL OF THE ROBOT

Symbol	Definition
f_{bw}	Friction force between body and wheel(N)
f_{wg}	Friction force between wheel and ground(N)
θ_p	Pitch angle of robot body(rad)
ϕ	Yaw angle of robot body(rad)
ψ	Tilt angle of robot body(rad)
$\theta_{m,r}$, $\theta_{m,l}$	Motor angle right and left(rad)
$\theta_{w,r}$, $\theta_{w,l}$	Wheel angle of right and left(rad)

Following (1), the contact point of the wheel (X_w, Y_w, Z_w) could be present as

$$(X_w, Y_w, Z_w) = (\int \dot{X}_w dt, \int \dot{Y}_w dt, 0) \tag{2}$$

The center of the axis (X_m, Y_m, Z_m) could be presented as

$$(X_m, Y_m, Z_m) = (X_w + r\sin\psi\sin\phi, Y_w - r\sin\psi\cos\phi, r\cos\psi) \tag{3}$$

The right and left wheel axis centers could be presented as

$$\begin{cases} (X_r, Y_r, Z_r) = (X_m + \frac{w}{2}\sin\phi, Y_m - \frac{w}{2}\cos\phi, Z_m) \\ (X_l, Y_l, Z_l) = (X_m - \frac{w}{2}\sin\phi, Y_m + \frac{w}{2}\cos\phi, Z_m) \end{cases} \tag{4}$$

Then, the robot's body states can be expressed as

$$\begin{aligned} X_b &= X_m + (l_1\cos\psi + l_2)\sin\theta_p\cos\phi + l_1\sin\psi\sin\phi \\ Y_b &= Y_m + (l_1\cos\psi + l_2)\sin\theta_p\sin\phi - l_1\sin\psi\cos\phi \\ Z_b &= Z_m + (l_1\cos\psi + l_2)\cos\theta_p \end{aligned} \tag{5}$$

Next, the Lagrange equations of the whole robot body could be expressed as

$$\begin{aligned} &\frac{d}{dt}(\frac{\partial L}{\partial \dot{\theta}_w}) - \frac{\partial L}{\partial \theta_w} = F_{\theta_w} \\ &\frac{d}{dt}(\frac{\partial L}{\partial \dot{\theta}_p}) - \frac{\partial L}{\partial \theta_p} = F_{\theta_p} \\ &\frac{d}{dt}(\frac{\partial L}{\partial \dot{\phi}_p}) - \frac{\partial L}{\partial \phi_p} = F_{\phi} \\ &\frac{d}{dt}(\frac{\partial L}{\partial \dot{\psi}}) - \frac{\partial L}{\partial \psi} = F_{\psi} \end{aligned} \tag{6}$$

The translational energy T_1, the rotational energy T_2, and the potential energy U are shown as follows.

$$\begin{aligned} T_1 &= \tfrac{1}{2}m(\dot{X}_r^2 + \dot{Y}_r^2 + \dot{Z}_r^2 + \dot{X}_l^2 + \dot{Y}_l^2 + \dot{Z}_l^2) + \tfrac{1}{2}M(\dot{X}_b^2 + \dot{Y}_b^2 + \dot{Z}_b^2) \\ &= m(r^2\dot{\theta}_w^2 + r^2\dot{\psi}^2 + \tfrac{W^2}{4}\dot{\phi}^2 + r^2\sin^2\psi\dot{\phi}^2 + 2r^2\sin\psi\dot{\theta}_w\dot{\phi}) \\ &\quad + \tfrac{1}{2}M[r^2\dot{\theta}_w^2 + r^2\dot{\psi}^2 + l_1^2\dot{\psi}^2 + 2l_1 r\cos^2\psi\dot{\psi}^2 + l_1^2\sin^2\psi\dot{\phi}^2 + 2rl_1\sin^2\psi\cos\theta_p\dot{\psi}^2 \\ &\quad + (l_1\cos\psi + l_2)^2\dot{\theta}_p^2 + (l_1\cos\psi + l_2)^2\sin^2\theta_p\dot{\phi}^2 + r^2\sin^2\psi\dot{\phi}^2 + 2r^2\sin\psi\dot{\theta}_w\dot{\phi} \\ &\quad + 2r(l_1\cos\psi + l_2)\cos\theta_p\dot{\theta}_w\dot{\theta}_p + 2l_1 r\sin\psi\dot{\theta}_w\dot{\phi} + 2r(l_1\cos\psi + l_2)\sin\psi\sin\theta_p\dot{\theta}_p\dot{\psi} \\ &\quad - 2rl_1\sin\psi\sin\theta_p\dot{\theta}_w\dot{\psi} - 2l_1(l1 + l2\cos\psi)\sin\theta_p\dot{\phi}\dot{\psi} \\ &\quad - 2r(l_1\cos\psi + l_2)\cos\psi\sin\theta_p\dot{\phi}\dot{\psi} - 2rl_1\sin\theta_p\sin^2\psi\dot{\phi}\dot{\psi} \\ &\quad + 2(r + l_1)(l_1\cos\psi + l_2)\cos\theta_p\sin\psi\dot{\phi}\dot{\theta}_p] \end{aligned}$$

$$\begin{aligned} T_2 &= \tfrac{1}{2}J_{wp}\dot{\theta}_r^2 + \tfrac{1}{2}J_{wp}\dot{\theta}_l^2 + \tfrac{1}{2}J_{wr}\dot{\psi}^2 + \tfrac{1}{2}J_{wr}\dot{\psi}^2 + \tfrac{1}{2}J_p\dot{\theta}_p^2 + \tfrac{1}{2}J_\phi\dot{\phi}^2 + \tfrac{1}{2}J_\psi\dot{\psi}^2 \quad (7) \\ &\quad + \tfrac{1}{2}n_1^2J_m(\dot{\theta}_{w,r} - \dot{\theta}_p)^2 + \tfrac{1}{2}n_1^2J_m(\dot{\theta}_{w,l} - \dot{\theta}_p)^2 + \tfrac{1}{2}n_2^2J_m\dot{\psi}^2 \\ &= \tfrac{1}{2}J_{wp}(2\dot{\theta}_w^2 + \tfrac{W^2}{2r^2}\dot{\phi}^2) + \tfrac{1}{2}J_{wr}\dot{\psi}^2 + \tfrac{1}{2}J_p\dot{\theta}_p^2 + \tfrac{1}{2}J_\psi\dot{\psi}^2 + \tfrac{1}{2}J_\phi\dot{\phi}^2 \quad (8) \\ &\quad + \tfrac{1}{2}n_1^2J_m(2\dot{\theta}_w^2 + \tfrac{W^2}{2r^2}\dot{\phi}^2 - 4\dot{\theta}_w\dot{\theta}_p + 2\dot{\theta}_p^2) + \tfrac{1}{2}n_2^2J_m\dot{\psi}^2 \end{aligned}$$

$$\begin{aligned} U &= mgZ_r + mgZ_l + MgZ_b \\ &= 2mgr\cos\psi + Mg(r\cos\psi + (l_1\cos\psi + l_2)\cos\theta_p) \end{aligned} \tag{9}$$

Substituting energy terms shown in (7)-(9) into (6), we could derive quantitative equations of motion of the system:

$$\begin{aligned} &\frac{d}{dt}(\frac{\partial L}{\partial \dot{\theta}_w}) - \frac{\partial L}{\partial \theta_w} = F_{\theta_w} \\ &\Rightarrow [(2m+M)r^2 + 2J_{wp} + 2n_1^2J_m]\ddot{\theta}_w + [Mr(l_1\cos\psi + l_2)\cos\theta_p - 2n_1^2J_m]\ddot{\theta}_p \\ &\quad + [(2m+M)r^2 + Mrl_1]\sin\psi\ddot{\phi} - Mrl_1\sin\theta_p\sin\psi\ddot{\psi} - Mr(l_1\cos\psi + l_2)\sin\theta_p\dot{\theta}_p^2 \\ &\quad - Mrl_1\sin\theta_p\cos\psi\dot{\psi}^2 - 2Mrl_1\cos\theta_p\sin\psi\dot{\theta}_p\dot{\psi} + [(2m+M)r^2 + Mrl_1]\cos\psi\dot{\phi}\dot{\psi} = F_{\theta_w} \end{aligned} \tag{10}$$

$$\begin{aligned} &\frac{d}{dt}(\frac{\partial L}{\partial \dot{\theta}_p}) - \frac{\partial L}{\partial \theta_p} = F_{\theta_p} \\ &\Rightarrow [Mr(l_1\cos\psi + l_2)\cos\theta_p - 2n_1^2J_m]\ddot{\theta}_w + [M(l_1\cos\psi + l_2)^2 + J_p + 2n_1^2J_m]\ddot{\theta}_p \\ &\quad + M(r + l_1)(l_1\cos\psi + l_2)\cos\theta_p\sin\psi\ddot{\phi} + Mr(l_1\cos\psi + l_2)\sin\theta_p\sin\psi\ddot{\psi} \\ &\quad - M(l_1\cos\psi + l_2)^2\sin\theta_p\cos\theta_p\dot{\phi}^2 + Mr(l_1\cos\psi + l_2)\sin\theta_p\cos\psi\dot{\psi}^2 \\ &\quad - 2M(l_1\cos\psi + l_2)l_1\sin\psi\dot{\theta}_p\dot{\psi} + 2M(r + l_1)(l_1\cos\psi + l_2)\cos\theta_p\cos\psi\dot{\phi}\dot{\psi} \\ &\quad - Mg(l_1\cos\psi + l_2)\sin\theta_p = F_{\theta_p} \end{aligned} \tag{11}$$

$$\begin{aligned} &\frac{d}{dt}(\frac{\partial L}{\partial \dot{\phi}_p}) - \frac{\partial L}{\partial \phi_p} = F_{\phi} \\ &\Rightarrow [(2m+M)r^2\sin\psi + Mrl_1\sin\psi]\ddot{\theta}_w + Mr(l_1\cos\psi + l_2)\cos\theta_p\sin\psi\ddot{\theta}_p \\ &\quad + [\tfrac{1}{2}mw^2 + 2mr^2\sin^2\psi + M(l_1\cos\psi + l_2)^2\sin^2\theta_p + M(r^2 + l_1^2)\sin^2\psi + J_\phi \\ &\quad + \tfrac{W^2}{2r^2}(J_{wp} + n_1^2J_m)]\ddot{\phi} - M(r + l_1)(l_1 + l_2\cos\psi)\sin\theta_p\ddot{\psi} \\ &\quad - M(r + l_1)(l_1\cos\psi + l_2)\sin\theta_p\sin\psi\dot{\theta}_p^2 + M(r + l_1)l_2\sin\theta_p\sin\psi\dot{\psi}^2 \\ &\quad + [2[(2m+M)r^2 + Ml_1^2]\sin\psi\cos\psi - 2M(l_1\cos\psi + l_2)l_1\sin\psi\sin^2\theta_p]\dot{\phi}\dot{\psi} \\ &\quad + 2M(l_1\cos\psi + l_2)^2\sin\theta_p\cos\theta_p\dot{\theta}_p\dot{\phi} - 2M(r + l_1)l_1\cos\theta_p\sin^2\psi\dot{\theta}_p\dot{\psi} \\ &\quad + [(2m+M)r^2 + Mrl_1]\cos\psi\dot{\theta}_w\dot{\psi} = F_{\phi} \end{aligned} \tag{12}$$

$$\begin{aligned} &\frac{d}{dt}(\frac{\partial L}{\partial \dot{\psi}}) - \frac{\partial L}{\partial \psi} = F_{\psi} \\ &\Rightarrow -Mrl_1\sin\theta_p\sin\psi\ddot{\theta}_w + Mr(l_1\cos\psi + l_2)\sin\theta_p\sin\psi\ddot{\theta}_p \\ &\quad - M(r + l_1)(l_1 + l_2\cos\psi)\sin\theta_p\ddot{\phi} \\ &\quad + [(2m+M)r^2 + Ml_1^2 + 2Mrl_1\sin^2\psi\cos\theta_p + 2Mrl_1\cos^2\psi + 2J_{wr} + J_\psi + n_2^2J_m]\ddot{\psi} \\ &\quad + [Mr(l_1\cos\psi + l_2)\cos\theta_p\sin\psi + M(l_1\cos\psi + l_2)l_1\sin\psi]\dot{\theta}_p^2 \\ &\quad + [M(l_1\cos\psi + l_2)l_1\sin^2\theta_p\sin\psi - [(2m+M)r^2 + Ml_1^2]\sin\psi\cos\psi]\dot{\phi}^2 \\ &\quad + 2Mrl_1(\cos\theta_p - 1)\sin\psi\cos\psi\dot{\psi}^2 - 2Mrl_1\sin^2\psi\sin\theta_p\dot{\theta}_p\dot{\psi} \\ &\quad - 2M(r + l_1)(l_1\cos\psi + l_2)\cos\theta_p\cos\psi\dot{\phi}\dot{\theta}_p - [(2m+M)r^2 + Mrl_1]\cos\psi\dot{\theta}_w\dot{\phi} \\ &\quad - 2mgr\sin\psi - Mg(r\sin\psi + l_1\sin\psi\cos\theta_p) = F_{\psi} \end{aligned} \tag{13}$$

In addition, the force terms could be presented as

$$
\begin{aligned}
F_{\theta_w} &= \alpha(V_r + V_l) - 2\beta\dot{\theta}_w + 2\beta\dot{\theta}_p \\
F_{\theta_p} &= -\alpha(V_r + V_l) + 2\beta\dot{\theta}_w - 2\beta\dot{\theta}_p \\
F_{\phi} &= -\tfrac{w}{2r}\alpha(V_r - V_l) - \tfrac{w^2}{2r^2}\beta\dot{\phi} - \tfrac{r+l_1}{r}\sin\psi[\alpha(V_r + V_l) - 2\beta\dot{\theta}_w + 2\beta\dot{\theta}_p] \\
F_{\psi} &= \gamma V_{tilt} - \xi\dot{\psi} \\
\alpha &= \frac{n_1 K_t}{R_m}, \quad \beta = \frac{n_1 K_t K_b}{R_m} + f_{bw} \\
\gamma &= \frac{n_2 K_t}{R_m}, \quad \zeta = \frac{n_2 K_t K_b}{R_m} + f_{bw}
\end{aligned} \tag{14}
$$

Note that non-linear terms of the dynamic equation are based on the robot pitch angle θ_p and the wheel speed θ_w which are mainly calculated in (10) and (11). The robot yaw and tilt angles are decided by (12) and (13). We linearize θ_p and ψ at the nominal balancing configuration (i.e., 0 radius/deg). Finally, the same state-space of the system as a standard 3D model can be yielded, as shown in (15). The LQR control is utilized to control the robot angle θ_p and test if different tilt angles ψ would affect balancing behavior.

$$
\dot{X} = \begin{bmatrix} \dot{\theta}_w \\ \dot{\theta}_p \\ \ddot{\theta}_w \\ \ddot{\theta}_p \end{bmatrix} = \underbrace{\begin{bmatrix} 0 & 0 & 1 & 0 \\ 0 & 0 & 0 & 1 \\ 0 & A(3,2) & A(3,3) & A(3,4) \\ 0 & A(4,2) & A(4,3) & A(4,4) \end{bmatrix}}_{A} \underbrace{\begin{bmatrix} \theta_p \\ \theta_w \\ \dot{\theta}_w \\ \dot{\theta}_p \end{bmatrix}}_{X} + \underbrace{\begin{bmatrix} 0 \\ 0 \\ B(3,1) \\ B(4,1) \end{bmatrix}}_{B} V_{in}
$$

$$
\begin{aligned}
A(3,2) &= -Mgl \times E(1,2) / \det(E) \\
A(3,3) &= [-(\beta + f_{wg}) \times E(2,2) - \beta \times E(1,2)] / \det(E) \\
A(3,4) &= [\beta \times E(2,2) + \beta \times E(1,2)] / \det(E) \\
A(4,2) &= -Mgl \times E(1,1) / \det(E) \\
A(4,3) &= [(\beta + f_{wg}) \times E(2,1) + \beta \times E(1,1)] / \det(E) \\
A(4,4) &= [-\beta \times E(2,1) - \beta \times E(1,1)] / \det(E)
\end{aligned}
$$

$$
\begin{aligned}
B(3,1) &= [\alpha \times E(2,2) + \alpha \times E(1,2)] / \det(E) \\
B(4,1) &= [-\alpha \times E(2,1) - \alpha \times E(1,1)] / \det(E)
\end{aligned}
$$

$$
E = \begin{bmatrix} (m+M)r^2 + J_w + n^2 J_m & Mrl - n^2 J_m \\ Mrl - n^2 J_m & Ml^2 + J_p + n^2 J_m \end{bmatrix} \tag{15}
$$

We consider a linearized model of (13) and rewrite it as state-space form and ignore 2nd order non-linear item as shown in (16):

$$
\dot{X}_2 = \begin{bmatrix} \dot{\psi} \\ \ddot{\psi} \end{bmatrix} = \underbrace{\begin{bmatrix} 0 & 1 \\ A_2(2,1) & A_2(2,2) \end{bmatrix}}_{A_2} \underbrace{\begin{bmatrix} \psi \\ \dot{\psi} \end{bmatrix}}_{X_2} + \underbrace{\begin{bmatrix} 0 \\ B_2(2,1) \end{bmatrix}}_{B_2} V_{tilt}
$$

$$
\begin{aligned}
\varepsilon &= (2m+M)r^2 + Ml_1^2 + 2J_{wr} + J_{\psi} + n_2^2 J_m \\
A_2(2,1) &= [2mgr + Mg(r + l_1)] / \varepsilon \\
A_2(2,2) &= -\zeta / \varepsilon \\
B_2(2,1) &= \gamma / \varepsilon
\end{aligned} \tag{16}
$$

Equation (16) reveals that another parameter could not affect the tilt angle. Because of the tilt mechanism of the worm drive system, we could quickly form a constant tilt angle to verify if the tilt angle affects balancing behavior.

IV. Experimental Evaluation of the Robot in Self-Balancing

The tiltable balancing robot was built for experimental validation, as shown in Fig. 1(a). The tilt mechanism and wheels are driven by 150W DC brushed motors with incremental encoders (RE40, MAXON). The main computer is a real-timed control system (PXI-8110 with I/O module PCI-7813R, National Instruments) running at 1kHz. A 1-axis rate gyro (ADXRS620, Analog Device) and a 2-axis inclinometer (SCA100T, VTI Technologies) are installed at the center of mass of the robot, providing the θ_p measurement for Kalman filter that gives self-balancing feedback signal. Wheel angle θ_w is measured by the motor's incremental encoder.

Before the experiments, MATLAB® was utilized to construct numerical solutions for the derived dynamic model and to design a self-balancing controller. The θ_w, θ_p and angular velocity states could converge to reference inputs. The simulation results will be shown with experimental data.

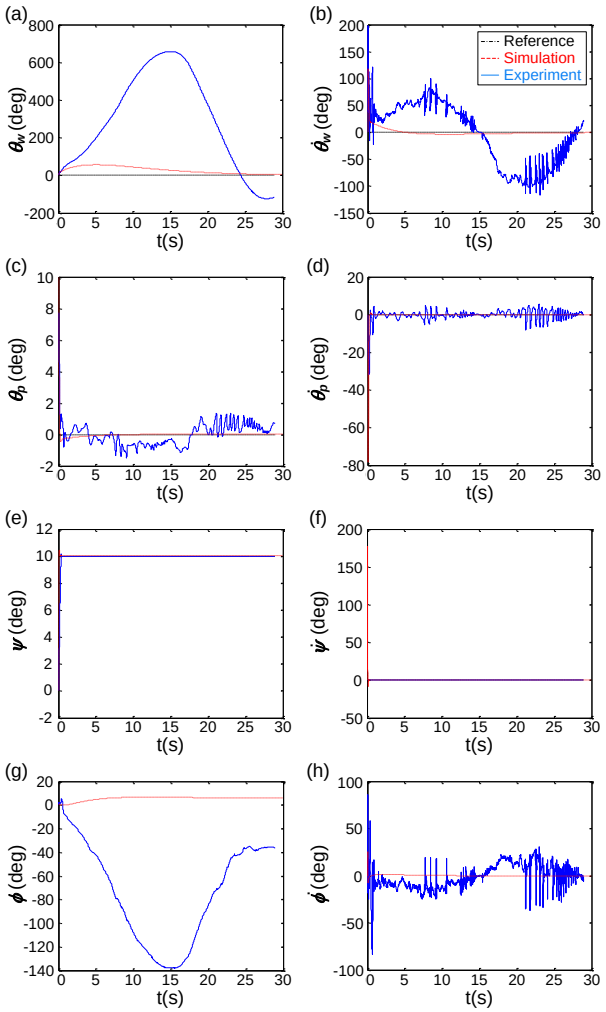

Fig. 3. The experimental results of the robot in self-balancing tests without forward moving. The left column and right column are states, as listed in TABLE II, and their derivatives.

In the balancing experiments, we focus on how the tilt angle would affect the balancing angle. As mentioned in Section II, the pitch angle θ_p and tilt angle could be described into two independent systems, so we use 2 separated LQR controller to control each system. The Q and R parameters are shown in (17).

$$Q_1 = \begin{bmatrix} 1 & 0 & 0 & 0 \\ 0 & 8\times10^6 & 0 & 0 \\ 0 & 0 & 1 & 0 \\ 0 & 0 & 0 & 1 \end{bmatrix}, R_1 = 10^3$$

$$Q_2 = \begin{bmatrix} 8\times10^6 & 0 \\ 0 & 1 \end{bmatrix}, R_2 = 10^3 \quad (17)$$

In equation (17), Q_1 and R_1 are LQR controller parameters of dynamic system of equation (15). We set a very larger value of θ_p to make sure it could converge to 0 radius/deg which is the linearized point as soon as possible.

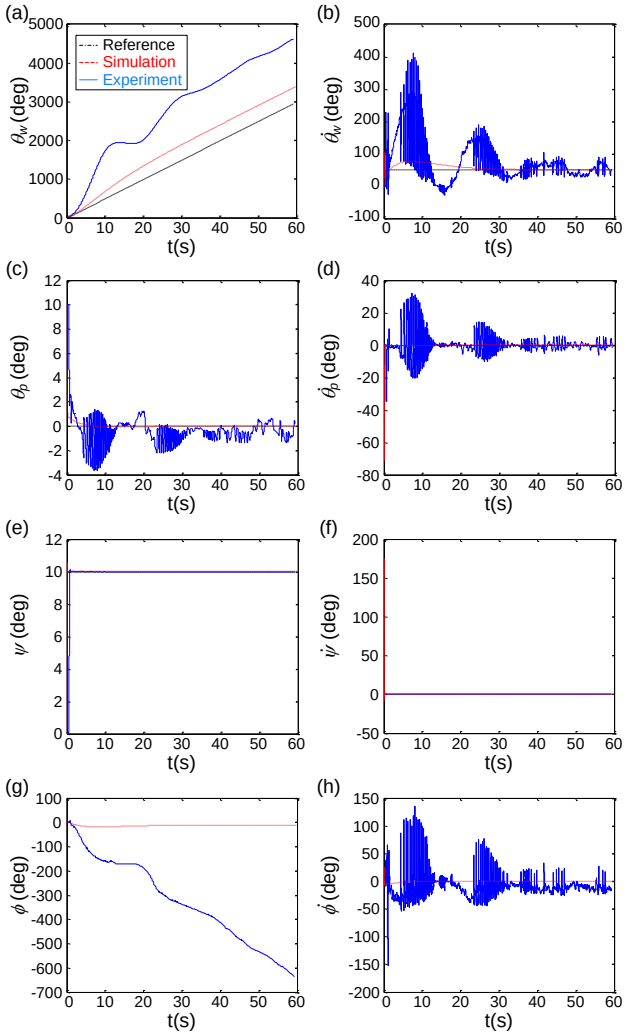

Fig. 4. The experimental results of the robot in self-balancing tests with forward moving. The left column and right column are states, as listed in TABLE I and their derivatives

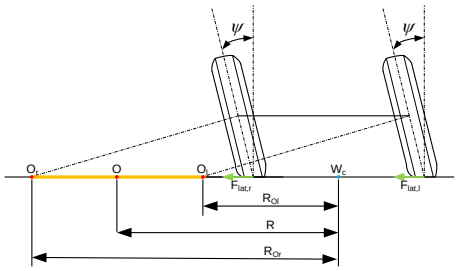

Fig. 5. The illustrative drawing of the robot in tilt configuration.

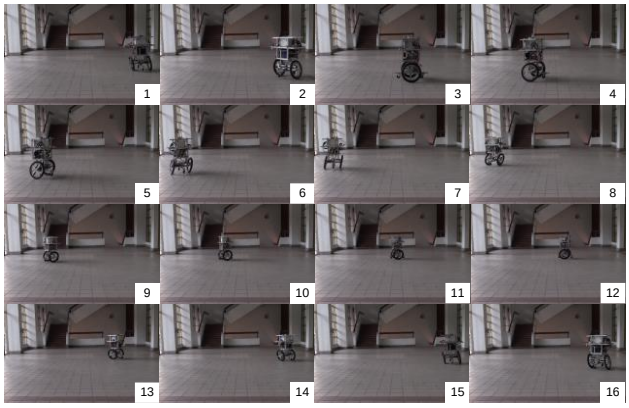

Fig. 6 The snapshots of the robot in turning with forward moving.

TABLE III

THE TURNING RADII AND TURNING SPEED OF THE ROBOT USING ACTIVE CONTROLLABLE LATERALLY TILTABLE MECHANISM

$\dot{\theta}_w$	ψ	R_{Or}	R_{Ol}	R
°/s	°	m	m	m
50	5	2.519	2.069	1.975
50	7.5	1.757	1.307	1.475
50	10	1.376	0.926	1.1
70	5	2.519	2.069	2.275
70	7.5	1.757	1.307	1.574
70	10	1.376	0.926	1.125

Q_2 and R_2 are LQR controller parameters of dynamic system of equation (16). We also set a large value of ψ to make it could converge as soon as possible to check if ψ could affect the balancing behavior.

In the first experiment, we tested θ_p from 10 deg to the self-balancing point of 0 deg and then controlled the tilt angle from 0 deg back to 10 deg. The result is shown in Fig. 3. The tilt angle ψ and the angular velocity could quickly converge to the reference input state. Meanwhile, body pitch angle θ_p also converges to 0 deg. This means that θ_p and ψ can be controlled separately. However, continuous self-balancing could cause a steady state of θ_w and ϕ, and their derivatives (i.e., angular velocities) would also have a steady-state error.

In the second experiment, we also start at θ_p from 10 deg but give a specific forward speed to check whether the system can achieve stable movement. The result is shown in Fig. 4. The main self-balancing state of θ_p, θ_w and their derivatives could achieve stable states with steady-state errors, similar to the simulation results. The tilt angle ψ would also converge to the reference input. In contrast, the angular velocity ϕ would have a state-steady error and cause a continuous body rotation.

According to the Theory of Ground Vehicles [26], this kind of situation is referred to as a camber, which would happen in a vehicle with a pneumatic tire. The model of our system with the chamber can be shown in Fig. 5. The contact point of the pneumatic tire and the ground would deform and cause a lateral force on the vehicle body, called camber thrust. The magnitude of camber thrust is related to tire pressure, the normal force on

the wheel, etc. Because of the camber thrust, the vehicle would rotate around point O, extending outward from the center of the wheel. But in our parallel four-bar linkage tilt mechanism design, the point O_r of the wheel right and the point O_l of the wheel left, would not be the same. The actual rotation center O would be located between O_r and O_l, which causes one wheel to slip. The ideal rotation radius of the wheel right and left could be present as (18).

$$R_{Or} = r/\sin\psi + \frac{w}{2}$$
$$R_{Ol} = r/\sin\psi - \frac{w}{2} \quad (18)$$

To validate the performance of the actively controllable tilt angle, we designed an experiment with a fixed wheel speed and a fixed tilt angle to check if the turning radii located at R_{or} and R_{ol}. As mentioned, at least one wheel would slip, so we could not measure the rotation radius directly from odometry. Thus, in the experiment, a camera was utilized to measure the rotation radius, as shown in Fig. 6. The results of turning radii are listed in TABLE III. We could observe that all rotation radii would be located between R_{or} and R_{ol}. As tilt angle ψ increase, R would get close to R_{or} because of the right wheel would have more normal force than the left wheel that would happen more slip than right wheel. From this experiment, we get a turning method by changing the tilt angle ψ.

V. Experimental Evaluation of the Robot in Turning

The relationship between the tilt angle and the robot's turning behavior was utilized to develop a turning strategy where the tilt angle control would not affect body self-balancing control. To evaluate the turning performance using a tiltable mechanism, the traditional turning strategy of the two-wheeled robot was also executed, which applies differential voltages to the wheel motors while keeping the summed voltage the same. Thus, the two wheels would generate different torques and actuate the robot to turn while not altering the forward motion.

Fig. 7 shows the experimental results. We set $\dot{\theta}_w$ to 50 °/s and use 2 different method, differential voltage of 0.5V and tilt angle of 10° to achieve robot turning.

The robot turning using differential voltages would yield an unstable turning speed. In addition, the range of pitch angle would be more extensive than normal movement. When the turning command was turned off, the balancing of the state of body pitch and wheel angle would cause vibration. In some situations, the body pitch could also not converge to a stable state. In contrast, the robot turning using the tilt mechanism yielded the same performance as forward motion without turning. After the turning command was turned off for forward motion, the state transitions were also smooth. TABLE VI shows RMS between measurement and reference of 3 body states. There is not much difference in the RMS value when using tilt method. However, voltage turning method would cause a significantly larger RMS value.

The experimental results confirm the effectiveness of the robot's turning using the proposed tilt mechanism and control.

TABLE VI
RMS of Tilt and Voltage Method

State	Tilt Method		Voltage Method	
	On	Off	On	Off
$\dot{\theta}_w$(°/s)	14.86	14.42	52.62	84.36
θ_p(°)	0.66	0.60	1.66	1.14
$\dot{\theta}_p$(°/s)	2.60	2.01	2.74	6.44

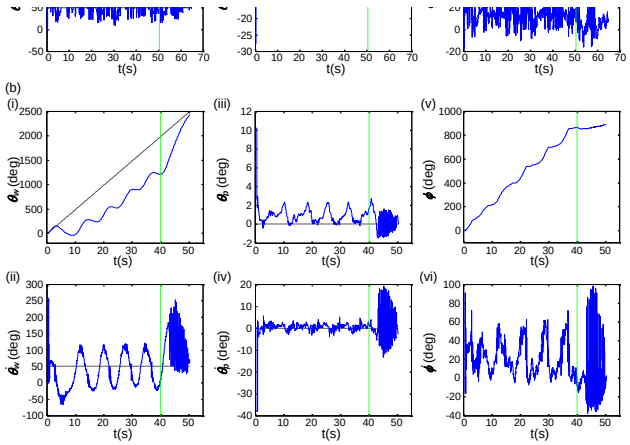

Fig. 7 Constant forward speed turning speed comparison (a) tilt angle (b) different voltage

VI. Conclusion

The traditional two-wheeled robots achieve body pitch angle control and movement using only two motors to fulfill the requirement of personal vehicles as well as to reduce the weight and the complex transmission systems. The wheel motors not only manage the body posture but also yield forward movement. This under-actuated design generates challenges for controller design. In this case, a simplified inverted pendulum model is utilized to achieve self-balancing. Owing to the high center of mass characteristics, the lateral overturning may occur. Thus, an actively controllable for tilting the robot laterally, can stabilize the robot.

This work advances the self-balancing two-wheeled robot by introducing an active tilt mechanism. By analyzing the dynamics, two independent controller systems of the robot's pitch angle and tilt angle are obtained. The unmodeled dynamics of the tilt wheels are utilized as a turning strategy. Due to the non-back drivable tilt mechanism design, self-balancing and turning control could be achieved as separate systems. The experimental results confirm the effectiveness of the tiltable mechanism in the robot turning.

References

[1] Y. Ha and S. Yuta, "Trajectory tracking control for navigation of self-contained mobile inverse pendulum," in *Intelligent Robots and Systems '94. 'Advanced Robotic Systems and the Real World', IROS '94. Proceedings of the IEEE/RSJ/GI International Conference on*, 12-16 Sep 1994 1994, vol. 3, pp. 1875-1882 vol.3, doi: 10.1109/iros.1994.407604.

[2] Y. S. Ha and S. Yuta, "Trajectory tracking control for navigation of the inverse pendulum type self-contained mobile robot," (in English), *Robot. Auton. Syst.*, Article; Proceedings Paper vol. 17, no. 1-2, pp. 65-80, Apr 1996, doi: 10.1016/0921-8890(95)00062-3.

[3] F. Grasser, A. D'Arrigo, S. Colombi, and A. C. Rufer, "JOE: a mobile, inverted pendulum," *Industrial Electronics, IEEE Transactions on*, vol. 49, no. 1, pp. 107-114, 2002, doi: 10.1109/41.982254.

[4] V. Coelho, S. Liew, K. Stol, and G. Liu, "Development of a Mobile Two-Wheel Balancing Platform for Autonomous Applications," in *Mechatronics and Machine Vision in Practice, 2008. M2VIP 2008. 15th International Conference on*, 2-4 Dec. 2008 2008, pp. 575-580, doi: 10.1109/mmvip.2008.4749594.

[5] K. Pathak, J. Franch, and S. K. Agrawal, "Velocity and position control of a wheeled inverted pendulum by partial feedback linearization," *Robotics, IEEE Transactions on*, vol. 21, no. 3, pp. 505-513, 2005, doi: 10.1109/tro.2004.840905.

[6] T. Takei, R. Imamura, and S. Yuta, "Baggage Transportation and Navigation by a Wheeled Inverted Pendulum Mobile Robot," *Industrial Electronics, IEEE Transactions on*, vol. 56, no. 10, pp. 3985-3994, 2009, doi: 10.1109/tie.2009.2027252.

[7] C. C. Tsai, H. C. Huang, and S. C. Lin, "Adaptive Neural Network Control of a Self-Balancing Two-Wheeled Scooter," *IEEE Transactions on Industrial Electronics*, vol. 57, no. 4, pp. 1420-1428, 2010, doi: 10.1109/TIE.2009.2039452.

[8] H. Jian, G. Zhi-Hong, T. Matsuno, T. Fukuda, and K. Sekiyama, "Sliding-Mode Velocity Control of Mobile-Wheeled Inverted-Pendulum Systems," *Robotics, IEEE Transactions on*, vol. 26, no. 4, pp. 750-758, 2010, doi: 10.1109/tro.2010.2053732.

[9] C.-C. Y. Ching-Chih Tsai, Shih-Min Hsieh, Feng-Chun Tai, "Intelligent Adaptive Simultaneous Tracking and Stabilization Using Fuzzy Wavelet Networks for a Wheeled Inverted Pendulum," *International Journal of iRobotics*, vol. 2, pp. 1-12, 2019.

[10] T. J. Ren, T. C. Chen, and C. J. Chen, "Motion control for a two-wheeled vehicle using a self-tuning PID controller," (in English), *Control Eng. Practice*, Article vol. 16, no. 3, pp. 365-375, Mar 2008, doi: 10.1016/j.conengprac.2007.05.007.

[11] C. H. Huang, W. J. Wang, and C. H. Chiu, "Design and Implementation of Fuzzy Control on a Two-Wheel Inverted Pendulum," *IEEE Transactions on Industrial Electronics*, vol. 58, no. 7, pp. 2988-3001, 2011, doi: 10.1109/TIE.2010.2069076.

[12] H.-T. H. Gwo-Ruey Yu, "Self-Balance Control of a Two-Wheeled Robot Using Polynomial Fuzzy Systems," *International Journal of iRobotics*, vol. 1, pp. 26-34, 2018.

[13] SEGWAY. http://www.segway.com/ (accessed.

[14] R. Hibbard and D. Karnopp, "Twenty first century transportation system solutions - A new type of small, relatively tall and narrow active tilting commuter vehicle," (in English), *Veh. Syst. Dyn.*, Article vol. 25, no. 5, pp. 321-347, May 1996, doi: 10.1080/00423119608968970.

[15] J. Gohl, R. Rajamani, L. Alexander, and P. Starr, "Active roll mode control implementation on a narrow tilting vehicle," (in English), *Veh. Syst. Dyn.*, Article vol. 42, no. 5, pp. 347-372, Nov 2004, doi: 10.1080/0042311042000266810.

[16] J. C. Chiou and C. L. Chen, "Modeling and Verification of a Diamond-Shape Narrow-Tilting Vehicle," *IEEE/ASME Transactions on Mechatronics*, vol. 13, no. 6, pp. 678-691, 2008, doi: 10.1109/TMECH.2008.2004769.

[17] S. Kwon, S. Kim, and J. Yu, "Tilting-Type Balancing Mobile Robot Platform for Enhancing Lateral Stability," *IEEE/ASME Transactions on Mechatronics*, vol. 20, no. 3, pp. 1470-1481, 2015, doi: 10.1109/TMECH.2014.2364204.

[18] D. B. Pham *et al.*, "Balancing and Tracking Control of Ballbot Mobile Robots Using a Novel Synchronization Controller Along With Online System Identification," *IEEE Transactions on Industrial Electronics*, vol. 70, no. 1, pp. 657-668, 2023, doi: 10.1109/TIE.2022.3146642.

[19] S. G. So and D. Karnopp, "Active dual mode tilt control for narrow ground vehicles," (in English), *Veh. Syst. Dyn.*, Article vol. 27, no. 1, pp. 19-36, Jan 1997, doi: 10.1080/00423119708969321.

[20] D. Piyabongkarn, T. Keviczky, and R. Rajamani, "Active direct tilt control for stability enhancement of a narrow commuter vehicle," (in English), *Int. J. Automot. Technol.*, Article vol. 5, no. 2, pp. 77-88, Jun 2004. [Online]. Available: <Go to ISI>://WOS:000221856600002.

[21] S. Kidane, R. Rajamani, L. Alexander, P. J. Starr, and M. Donath, "Development and Experimental Evaluation of a Tilt Stability Control System for Narrow Commuter Vehicles," *Control Systems Technology, IEEE Transactions on*, vol. 18, no. 6, pp. 1266-1279, 2010, doi: 10.1109/tcst.2009.2035819.

[22] J. Berote, J. Darling, and A. Plummer, "Development of a tilt control method for a narrow-track three-wheeled vehicle," (in English), *Proc. Inst. Mech. Eng. Part D-J. Automob. Eng.*, Article vol. 226, no. D1, pp. 48-69, 2012, doi: 10.1177/0954407011412311.

[23] S. Kim, J. Seo, and S. Kwon, "Development of a two-wheeled mobile tilting & balancing (MTB) robot," in *2011 11th International Conference on Control, Automation and Systems*, 26-29 Oct. 2011 2011, pp. 1-6.

[24] G. A. Muñoz-Hernandez, J. Díaz-Téllez, J. Estevez-Carreon, and R. S. García-Ramírez, "ADRC Attitude Controller Based on ROS for a Two-Wheeled Self-Balancing Mobile Robot," *IEEE Access*, vol. 11, pp. 94636-94646, 2023, doi: 10.1109/ACCESS.2023.3308948.

[25] Y. Yamamoto, "NXTway-GS Model-Based Design - Control of self-balancing two-wheeled robot built with LEGO Mindstorms NXT - ". [Online]. Available: http://www.pages.drexel.edu/~dml46/Tutorials/BalancingBot/files/NXTway-GS%20Model-Based_Design.pdf

[26] J. Y. Wong, *Theory of Ground Vehicles*, Third Edition ed. 2001, p. 4.

Wei-Shun Yu received the B.S. and M.S degrees in mechanical engineering from National Taiwan University, Taipei, Taiwan, in 2010 and 2012, respectively. He was a robot firmware engineer at Kinpo Electronics, Inc from 2014 to 2017. Also He worked as an automation robotics engineer at LNC from 2018 to 2019. He is currently a research assistant at the Department of Mechanical Engineering, National Taiwan University, Taipei, Taiwan.

His areas of interest include mechatronics, automation systems, and robot control firmware.

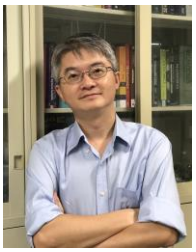

Pei-Chun Lin received the B.S. and M.S. degrees in mechanical engineering from National Taiwan University, Taipei, Taiwan, in 1996 and 1998, respectively, and the M.S. degree in electrical engineering and computer science and the Ph.D. degree in mechanical engineering from the University of Michigan, Ann Arbor, MI, USA in 2005. He was a Postdoctoral Research Fellow with the Department of Materials Science and Engineering, University of Pennsylvania, Philadelphia, PA, USA, from 2005 to 2007. He is currently a Distinguished Professor at the Department of Mechanical Engineering, National Taiwan University, Taipei, Taiwan.

His research interests include bio-inspired robotics, mechanism design, mechatronics, control, and dynamic locomotion.